

# Microstructural evolution in silica aerogel

Carlos Folgar <sup>\*</sup>, Diane Folz, Carlos Suchicital, David Clark

*Department of Materials Science and Engineering, Virginia Polytechnic Institute and State University, Blacksburg, VA 24061, USA*

Received 11 August 2006; received in revised form 6 February 2007

Available online 9 April 2007

## Abstract

Microstructural evolution in silica aerogel has been observed in samples produced by the hydrolysis and polycondensation of tetramethylorthosilicate that was acid catalyzed. Drying of the silica gel was performed by replacing its liquid phase with liquid carbon dioxide, which was removed under high pressure and low temperature conditions in a critical point dryer. Different stages of microstructural evolution have been observed through a thermal process from room temperature to 1500 °C in a conventional furnace. In addition, microstructural characterization has been performed using nitrogen adsorption, helium pycnometry, Fourier transform infrared spectroscopy, X-ray diffraction and thermogravimetric analysis. The primary goal of this work is to fully understand the microstructural evolution of silica gel so it may be used more extensively in developing ceramic materials with novel, designed microstructures.

© 2007 Elsevier B.V. All rights reserved.

PACS: 82.33.Ln; 81.20.Fw; 81.05.Rm; 61.43.Gt

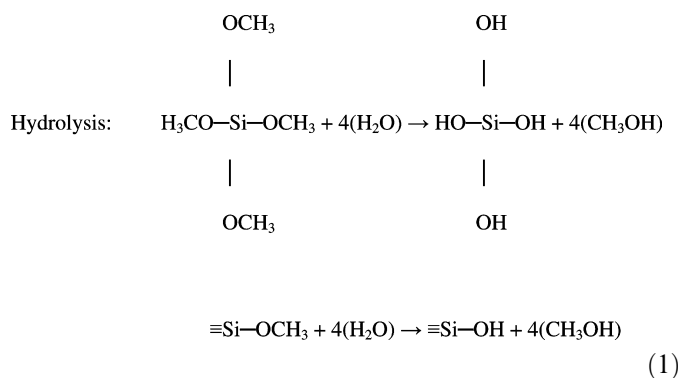
Keywords: Porosity; Silica; Sol–gel, aerogel and solution chemistry; Aerogels; Sol–gels (xerogels)

## 1. Introduction

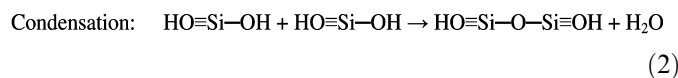
There is a rising demand for new materials for use in many fields of technology, including electronic, optic and energy storage devices. They require rigorously controlled compositions and purities as well as sophisticated processing to achieve specifically designed microstructures. Some of the critical aspects required in developing new materials include designing process parameters and controlling microstructure development. Sol–gel processing lends itself to these tasks due to the ease of stoichiometric control [1,2]. These new materials may present unique microstructures and corresponding bulk properties. A particular interest of this work has been to fully understand the microstructural evolution of silica gel in order to tailor specific ceramic materials with novel microstructures.

The method described in this paper for making monolithic silica gel involves hydrolysis and polycondensation of organometallic compounds, such as silicon alkoxides

(e.g., tetramethyl orthosilicate, TMOS) [3]. Once TMOS ( $\text{Si}(\text{OCH}_3)_4$ ) is mixed with water, hydrolysis occurs as indicated by the following reaction:



The silica hydroxyl groups interact with each other to produce siloxane bonds ( $\equiv\text{O-Si-O}\equiv$ ). This interaction is known as condensation (Eq. 2).

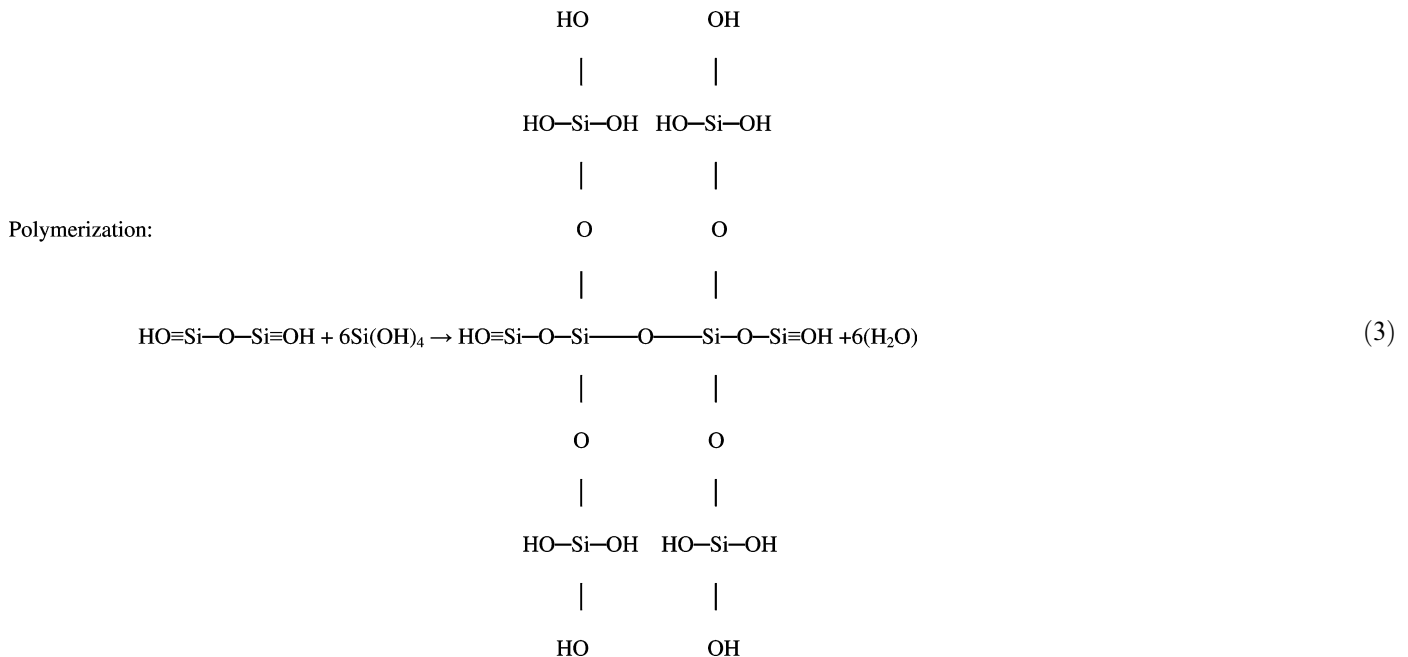


<sup>\*</sup> Corresponding author.

E-mail address: [cfolgar@vt.edu](mailto:cfolgar@vt.edu) (C. Folgar).

The condensation continues, forming a three-dimensional network through a reaction known as polymerization (Eq. 3).

It is well known from the literature that the microstructure of dried silica gel changes significantly when it is heated in a conventional oven/furnace [6,8]. Generally, a



After the partially polymerized sol in Eq. (3) is cast, polymerization continues resulting in gelation. This reaction continues even after gelation through aging and is one of the factors that influences the evolution of the microstructure. The wet gel is then dried using one of several techniques, such as the process used to make xerogel or aerogel.

A xerogel is produced when the wet solid material is dried in a conventional oven over long process times [4]. The xerogel is susceptible to cracking due to the capillary pressure developed during the drying process.

An aerogel is produced when the liquid is removed as a gas phase from the interconnected solid matrix after passing through hypercritical conditions [5]. This process reduces the capillary pressure, and it is much easier to obtain a large bulk sample than by using the xerogel process. Aerogels have very low density, high porosity, low thermal conductivity and a low dielectric constant [6]. They can be manufactured by two different processes: one requires high temperature and high pressure because the solvent used is passed through its critical point; the other requires low temperature and high pressure. In this work, the latter was used and required that the solvent be replaced by liquid carbon dioxide (CO<sub>2</sub>), at about 5 °C. Critical conditions (~32 °C, ~73 atm) of the new liquid phase were reached as the temperature increased. The microstructural modification of silica gel could be minimized by taking particular care during the solvent exchange procedure in the drying process [4,7].

dried silica gel consists of an amorphous silica matrix containing a distribution of pore sizes. Several stages of evolution are observed when silica gel is heated conventionally.

- Stage I: drying and stabilization. The pore volume is slightly reduced by eliminating the small pores and no significant structural changes are observed (25–700 °C).
- Stage II: dehydration and partial densification. There is a substantial decrease in pore volume due to the reduction of large pores, and a narrow distribution of pore sizes is observed (700–1000 °C).
- Stage III: densification. The elimination of porosity is completed (1000–1200 °C).
- Stage IV: nucleation and partial crystallization is observed (1200–1300 °C).
- Stage V: crystallization and growth. This evolution depends on the chemical and physical parameters involved in its composition and the thermal process used for its preparation [9–11].

In this paper, we focus on the microstructural evolution in silica aerogel through a thermal treatment in a conventional oven, and the mechanisms that influence its evolution.

## 2. Experimental procedure

Silica aerogel samples were produced with an average pore size distribution (diameter = 130 Å) by following a

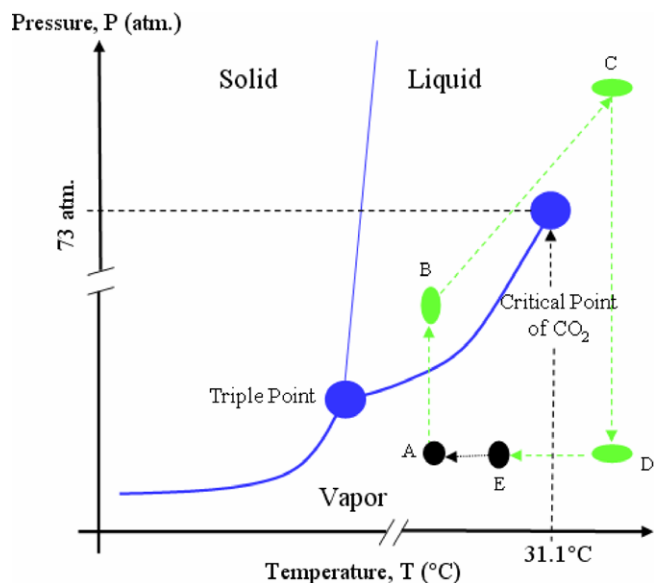


Fig. 1. Drying process of aerogel is presented on the phase diagram of  $\text{CO}_2$ .

standard procedure using TMOS combined with a mixture of dilute nitric acid ( $\text{HNO}_3$ ) and dilute hydrofluoric acid (HF) as catalysts (0.6 and 0.2 vol.%, respectively) [3]. These starting materials were mixed and then cast into polypropylene containers, which were sealed and kept at room temperature for eight hours (resulting in gelation). The samples were then placed in a larger container and allowed to age for six days in ethanol ( $\text{C}_2\text{H}_5\text{OH}$ ).

After aging, the silica gel samples were dried under specific pressure and temperature conditions according to the following procedure (the path followed is shown in capital letters in Fig. 1):

- The wet gel and  $\text{C}_2\text{H}_5\text{OH}$  were loaded into a critical point dryer unit (CPD)<sup>1</sup> at 5 °C, and the chamber was filled with liquid  $\text{CO}_2$  (A–B).
- The solvent,  $\text{C}_2\text{H}_5\text{OH}$ , was removed by repeated purging while keeping the chamber full of  $\text{CO}_2$  (B).
- While the chamber temperature was slowly raised above the critical temperature (31 °C), the pressure increased (B–C).
- When the pressure was greater than 73 atm, the  $\text{CO}_2$  passed into a supercritical fluid. Subsequently, the pressure was brought below 73 atm and the supercritical fluid passed to gas. The gas in the chamber was vented gradually (C–D), and the temperature was brought down slowly to ambient temperature (D–E).

An example of a dried silica aerogel produced in this manner is shown in Fig. 2. The fogginess of the sample is due to the high degree of porosity [5]. Monolithic samples received a thermal treatment at ambient pressure in air for

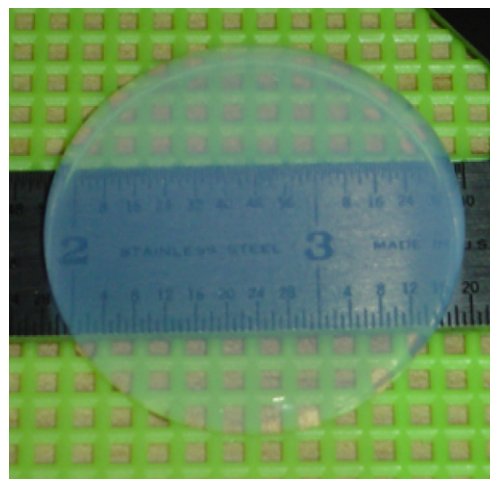


Fig. 2. Monolithic silica aerogel dried in a CPD with  $\text{CO}_2$ .

30 min at a predetermined temperature using a conventional furnace<sup>2</sup> and then were characterized.

Different techniques were used to characterize the aerogel samples. Pore volume, surface area and pore size distribution were analyzed using a nitrogen adsorption/desorption system.<sup>3</sup> Helium pycnometry<sup>4</sup> was carried out on all the samples to obtain the structural density of the silica network processed at different temperatures. Fourier transform infrared spectrographs (FTIR)<sup>5</sup> were collected for all the samples. Thermal gravimetric analyses (TGA)<sup>6</sup> and X-ray diffraction analyses (XRD)<sup>7</sup> were performed on selected samples.

### 3. Results

Pore volume and surface area evolutions obtained from adsorption analysis on samples at different temperatures are shown in Fig. 3(a). Both curves exhibit similar behavior. It is observed that the pore volume evolution of the aerogel undergoes a slow increase until around 300 °C, then a rapid decrease until 1100 °C, where the pore volume nearly disappears at higher temperatures (>1100 °C). In order to observe a possible tendency, the points plotted in Fig. 3 are joined by a line. The same methodology has been followed in Figs. 5 and 9.

The distribution of pore size obtained from nitrogen adsorption at different temperatures is presented in Fig. 4. As the temperature increases, the distribution tends to become concentrated in the smaller sizes, but it is not as narrow in a specific size as is observed in other types of silica gels, such as some acid-catalyzed xerogels [12].

<sup>2</sup> CM Furnace.

<sup>3</sup> Quantachrome Corporation, Autosorb 1.

<sup>4</sup> Micromeritics, AccuPyc 1330.

<sup>5</sup> TEC, Nicolet Avatar.

<sup>6</sup> NETZSCH, Jupiter.

<sup>7</sup> SCINTAG INC., XDS 2000.

<sup>1</sup> Quorum Technologies, T3000.

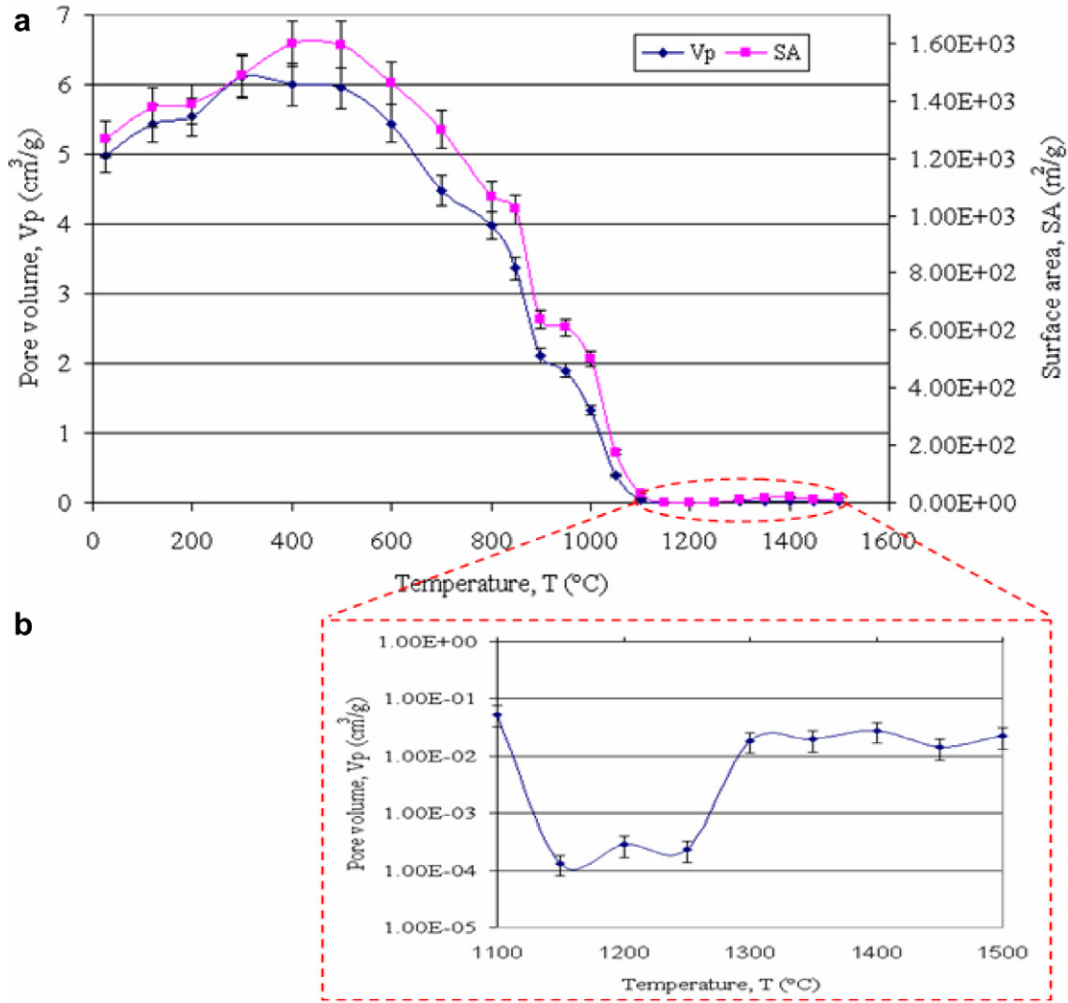


Fig. 3. Pore volume and surface area evolution of aerogel (a) temperature range between  $T_{\text{amb}}$  and 1500 °C; (b) temperature range between 1100 °C and 1500 °C.

Structural density at different temperatures is shown in Fig. 5. The structural density of the aerogel increases by about 25% from the as-dried sample to the sample fired at 1200 °C, with a maximum value of 2.227 g/cm<sup>3</sup>. The graph has been divided into six regions. Region I does not present significant changes in density (25–300 °C). Region II ranges from 300 to 600 °C and shows a rapid increase in density (16%). Region III describes a slow increase until around 1000 °C. Region IV lies between 1000 and 1250 °C and reveals a very small variation. Region V shows a reduction in the structural density (1250–1400 °C) and, beyond that, Region VI increases to nearly the maximum value observed in Region IV.

Fig. 6 shows FTIR transmission spectra of the aerogel densified at different temperatures. The bands observed for the silica aerogel, summarized in Table 1, are typical of sol-gel silica [13]. It has been observed that as the samples densified at higher temperatures, the position of the peak maximum ( $P_m$ , the peak occurring between 1025 and 1125 cm<sup>-1</sup>) is shifted to higher values within the range from room temperature to 1300 °C whose maximum value

falls at 1123 cm<sup>-1</sup>. However, the position of  $P_m$  at 1500 °C is lower than the one at 1300 °C.

The results of the weight loss for aerogel as dried to 1500 °C at a constant heating rate of 5 °C/min in a nitrogen atmosphere are presented in Fig. 7. The TGA curve reveals five different regions. Region I shows a sharp decrease in weight when the sample is heated up from room temperature to almost 200 °C, with a weight loss of about 11%. Region II lies between 200 and 300 °C and is associated with a small weight loss of about 1%. Region III falls between 300 and 600 °C and reveals a weight loss of approximately 5%. Region IV lies between 600 and 1250 °C accounting for a weight loss of around 3%. Finally, Region V describes a constant weight after 1250 °C. As a result, a total weight loss of approximately 20% was reached between room temperature and 1500 °C.

Typical XRDs of two samples heated at 1300 °C for 30 min and 1 h. are presented in Fig. 8(a) and (b), respectively. Fig. 8(b) shows that silica aerogel may begin a new phase change. This change could be time-dependent

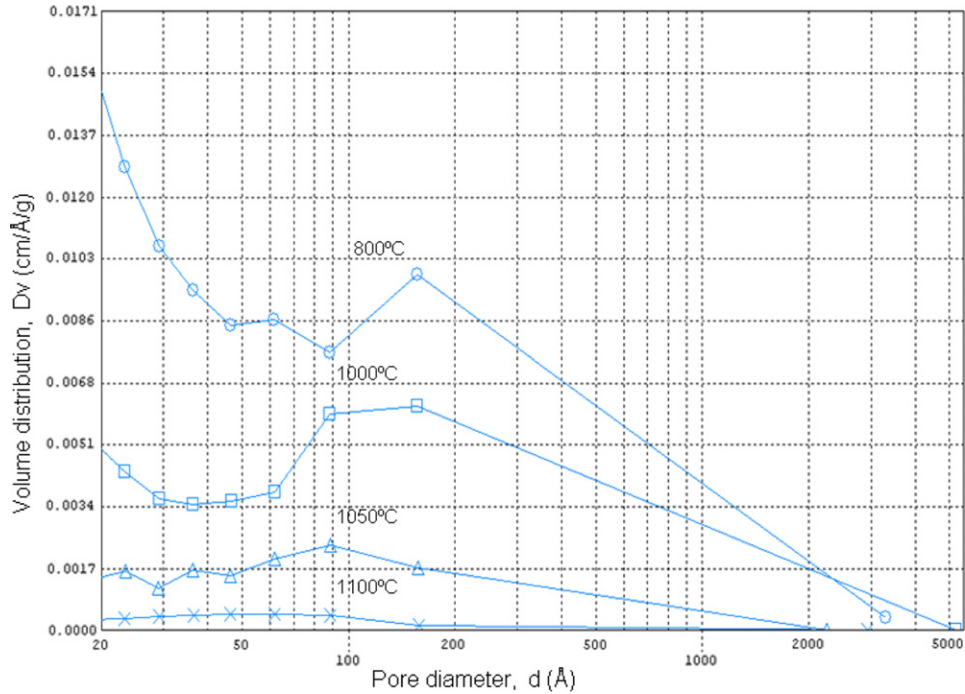


Fig. 4. Pore size distribution of aerogel at different temperatures obtained by nitrogen adsorption.

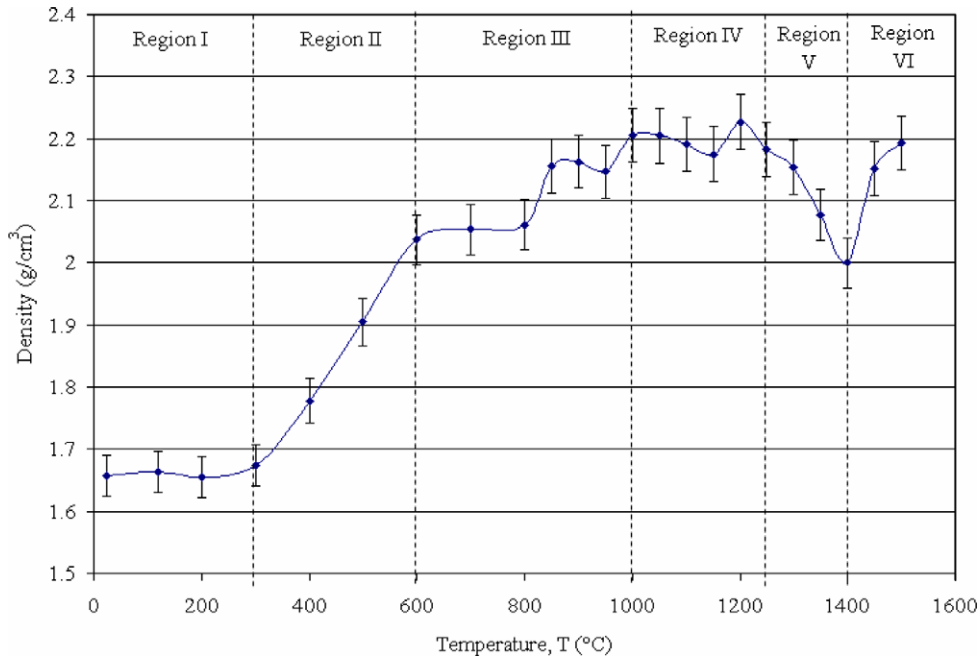


Fig. 5. Structural density measured by helium pycnometry of aerogel samples heat treated at different temperatures.

because the XRD at the same temperature for 30 min presents an amorphous structure (Fig. 8(a)).

#### 4. Discussion

From the pore volume ( $V_p$ ) and surface area (SA) data for different temperatures, the hydraulic radius ( $r_h$ ) can be calculated from [14].

$$r_h = \frac{2 V_p}{SA} \tag{4}$$

The hydraulic radius represents an average pore radius (Fig. 9) and is used in this work to explain how the microstructure changes with temperature. This information can be divided into five regions which correlate to those in Fig. 5 and are discussed below.

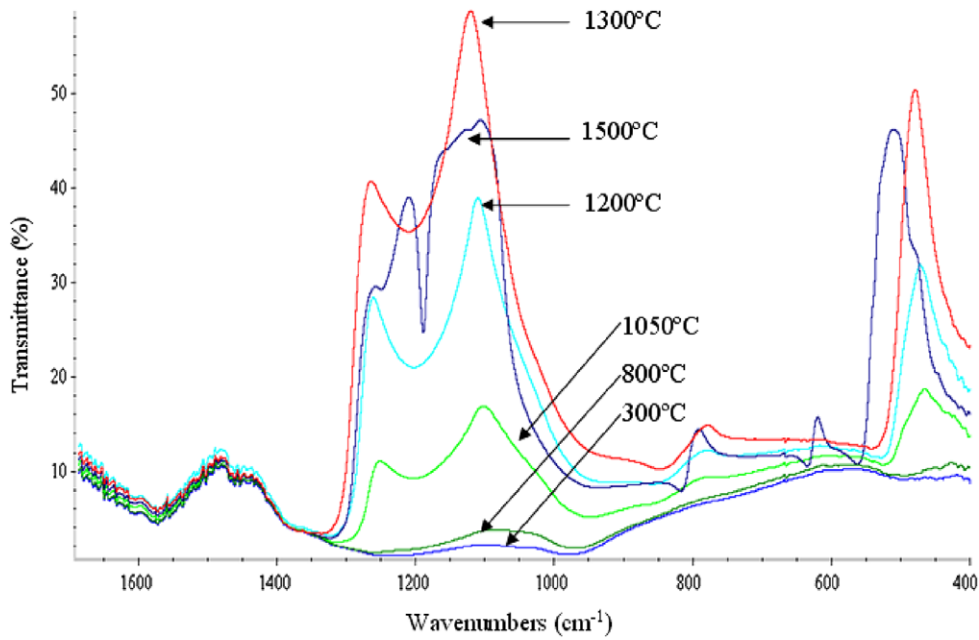


Fig. 6. FTIR transmittance spectra for aerogel at different temperatures.

Table 1  
FTIR bands observed for silica gel [13]

Frequency (cm <sup>-1</sup> )	Assignment
1640	Absorbed water (H <sub>2</sub> O)
1200	Asymmetric stretching (Si–O–Si)
960	Symmetric stretching (Si–OH)
795	Symmetric stretching (Si–O–Si)
460	Bending mode (O–Si–O)

4.1. Region I

This region ranges from room temperature to 300 °C and shows a small increase in  $r_h$ . Pore volume and surface area present a small variation while the structural density remains almost constant, as can be seen in Figs. 3 and 5, respectively. Thus no densification is associated with the apparent dilation observed at the beginning of the process. However, a considerable weight loss is observed (Fig. 7)

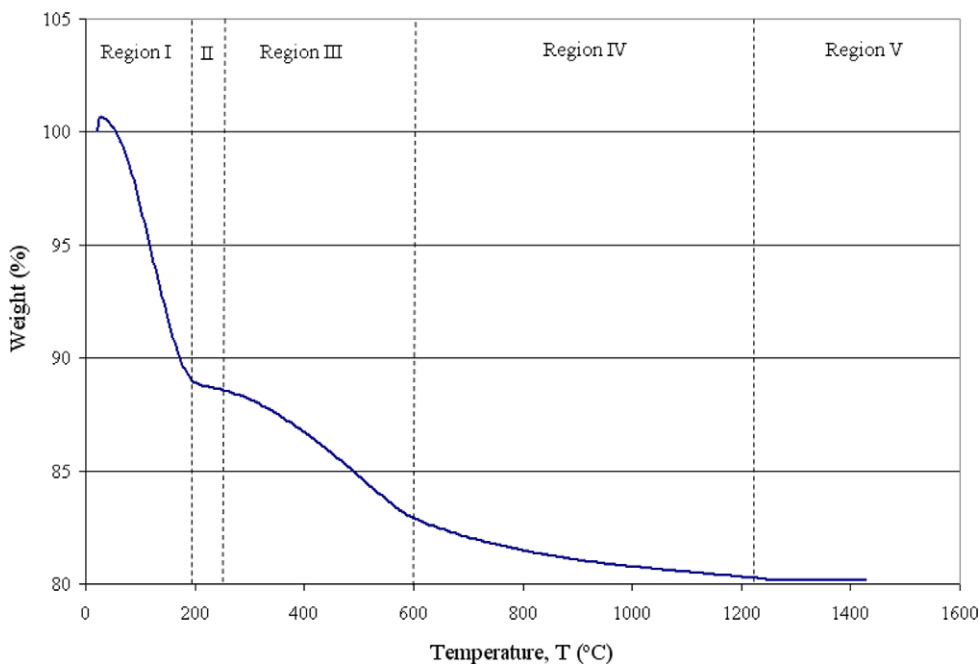


Fig. 7. Weight loss of aerogel heated at 20 °C/min in nitrogen as measured by TGA.

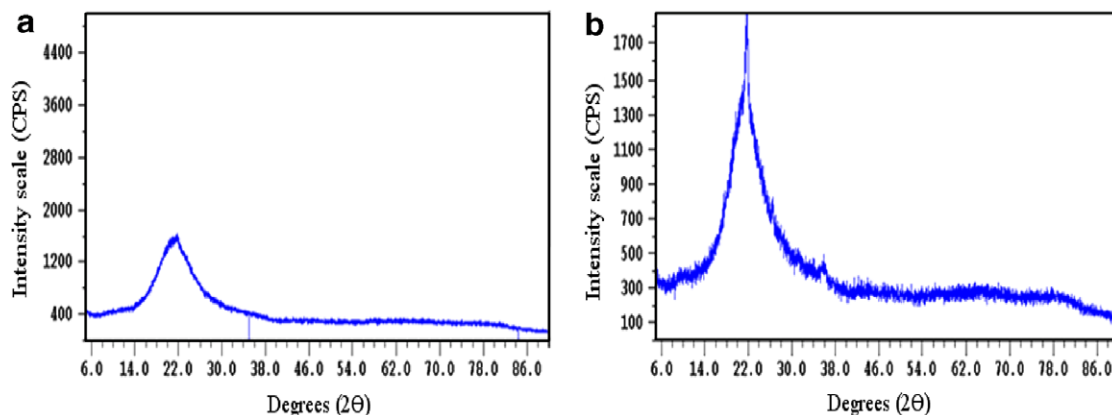


Fig. 8. XRD of silica gel fired at (a) 1300 °C for 30 min, and (b) 1300 °C for 1 h.

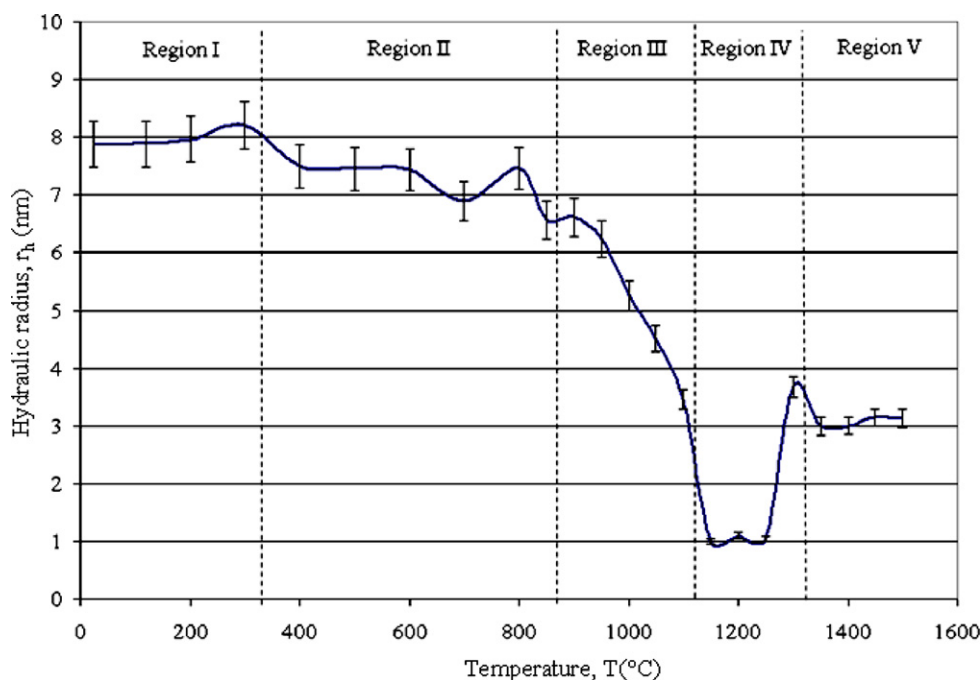


Fig. 9. Hydraulic radius of aerogel at different temperatures.

which can be associated with evaporation of physically absorbed water and perhaps the remains of ethanol. Consequently, desorption of these substances could be one of the main mechanisms for the dilatation observed in this region.

#### 4.2. Region II

This region lies between 300 and 850 °C and shows a slow decrease in  $r_h$ . In addition, slow decreases in  $V_p$  and SA are observed, accompanied by an increase of the density. This density variation is approximately 3/4 of the total density change (Fig. 5). The increase in structural density can be related to the weight loss observed (Fig. 7). Moreover, this weight loss could be correlated to evaporation of water formed from polycondensation reactions (Eqs. 2 and 3) and removal of organic groups by oxidation. However, oxidation of organic groups should not be related to

changes in  $V_p$  and SA, so the most probable mechanisms for these changes are structural relaxation, polycondensation reactions and classical sintering mechanisms that are responsible for rearranging the structure to minimize the surface area. Additionally, over this region, the dehydration stage begins and the presence of hydroxyls is found, which contributes to the reduction in viscosity of the material [15]. These two factors are significant mechanisms at the beginning of a sintering process.

#### 4.3. Region III

This region ranges from 850 to 1100 °C and indicates a rapid decrease in  $r_h$ . The gel abruptly changes its  $V_p$  and SA, revealing a decrease of  $V_p$  around 3.5 cm<sup>3</sup>/g which corresponds to 40% of the total change (Fig. 3(a)). Also, the TGA curve illustrates a small weight loss (Fig. 7),

and Fig. 5 shows a small increase in density from 850 to 950 °C followed by almost no change. Therefore, the rapid changes in  $V_p$  and SA without weight loss could be the result of viscous flow which allows the pores in the gel to collapse. These microstructural changes suggest that densification is taking place in this region.

#### 4.4. Region IV

This region ranges from 1100 to 1300 °C and presents the minimum  $r_h$  (1 nm). Variations in pore volume, surface area and weight loss are very small. Densification has reached its maximum in this region. The FTIR analyses of samples fired from 1200 to 1500 °C (Fig. 6) show how, as temperature increases, the position of the peak at  $1075\text{ cm}^{-1}$  is shifted to higher values. This peak corresponds to the asymmetric stretching vibration of Si–O–Si and can be interpreted as a measure of the densification. The structural density obtained in this region is slightly higher than the density of melted glass, indicating a structure more free of defects, as is pointed out in the literature [12,16]. Consequently, it can be said that the densification rate is inversely proportional to the pore diameter and high temperatures are needed to collapse large pores, as seen in Fig. 4. Even though the maximum density is reached in this region, the presence of very small pores may be possible. Very small pore volume can be observed in Fig. 3(b) at high temperatures, suggesting the possibility of closed pore masking. Also, a small decrease in  $V_p$  was measured in this range (Fig. 3(b)) which affects the size of the  $r_h$  as well.

#### 4.5. Region V

This region ranges from 1300 to 1500 °C and there is only a small variation of  $r_h$ . Almost constant behavior is observed in  $V_p$ , SA and weight loss; however, a decrease in density is observed (Fig. 5). Additionally, the Si–O–Si peak in the FTIR ( $1075\text{ cm}^{-1}$ ) is lower at 1500 °C and there is a slight increase in  $V_p$ , as observed (Fig. 3(b)). This behavior may be due to the beginning of a phase change in the material, probably nucleation. X-ray diffraction has been performed at 1300 °C for 1 h, as shown in Fig. 8, and silica is not completely amorphous. Some authors have indicated that silica gel type xerogels crystallize at 1300 °C after 2 h [17]. This behavior has not been observed in this case, but could occur at higher temperature or longer processing times.

## 5. Summary

Monolithic silica aerogel was prepared and then subjected to a thermal treatment to evaluate its microstructural evolution from room temperature to 1500 °C. The explanation of the observed phenomena was presented across five regions illustrated on the average pore radius ( $r_h$ ) graph at different temperatures.

Evaporation of physically absorbed water, and perhaps ethanol, dominates at low temperatures (Region I) which

increases pore volume and surface area approximately 20%. Oxidation of some organic residues is one of the main factors that generates about 6% of the total weight loss at intermediate temperatures (Region II), and the presence of the initial densification stages contributes to a decrease in surface area and pore volume. A reduction in pore size is observed at temperatures near 1000 °C (Region III and Region IV). The density slowly increases to its maximum value suggesting that densification occurs due to polycondensation reactions, structural relaxation and viscous flow have a strong influence over the material properties in these regions. Additionally, presence of nano-pores (pore diameters  $\leq 2\text{ nm}$ ) is found even at the highest density, which indicates the possibility of closed pore masking. At higher temperatures (Region V), a rearrangement of the structure is observed which may be due to the beginning of a new phase. Future work will be performed to analyze more precisely this behavior.

This study provides a proposed pathway of microstructural evolution for silica aerogel. It is expected that further applications in the technology associated with this gel may use this publication as a reference and lead to future, more extensive studies and discoveries.

## Acknowledgement

The authors would like to thank Ms. Ashley White, University of Cambridge, United Kingdom for her review of the materials presented in this paper.

## References

- [1] P.D. Maniar et al., *J. Non-Cryst. Solids* 124 (1990) 101.
- [2] W. Nie, G. Boulon, *J. Non-Cryst. Solids* 121 (1990) 282.
- [3] G.P. LaTorre, J.K. West, in: J.K. West, L.L. Hench (Eds.), *Chemical Processing of Advanced Materials*, Wiley, New York, 1992, p. 891.
- [4] A.E. Elias, in: *Materials Science and Engineering*, University of Florida, Gainesville, 1989, p. 172.
- [5] *Aerogels*, in: *Springer Processing in Physics*, Springer-Verlag, Heidelberg, 1986.
- [6] J. Fricke, T. Tillotson, *Thin Solid Films* 297 (1997) 212.
- [7] M. Casu, M. Casula, A. Corrias, G. Paschina, *J. Non-Cryst. Solids* 315 (2003) 97.
- [8] R.K. Iler, *The Chemistry of Silica*, John Wiley & Sons, 1979.
- [9] L.L. Hench, J.K. West, *Chem. Rev.* 90 (1990) 33.
- [10] J. Iura, H. Hishikura, M. Kamikatan, T. Kawaguchi, *J. Non-Cryst. Solids* 100 (1988) 241.
- [11] C. Folgar, D. Folz, C. Suchicital, D. Clark, *Drying silica-gel using microwaves*, in: R.L. Shulz, D.C. Folz (Eds.), *Microwaves and Radio Frequency Applications*, The Microwave Working Group, Ltd., Arnold, Maryland, 2004, pp. 166–173.
- [12] L.L. Hench, in: M.G.E. Bunshad, F. Rointan, M. Rosnagel Stephen (Eds.), *Sol–Gel Silica*, Materials Science and Process Technology Series, Noyes Publications, Westwood, 1998.
- [13] C.J. Brinker, G.W. Scherer, *Sol–Gel Science*, Academic Press, New York, 1990.
- [14] G.W. Scherer, D.M. Smith, *J. Non-Cryst. Solids* 189 (1995) 197.
- [15] F. Orgaz-Orgaz, *J. Non-Cryst. Solids* 100 (1988) 115.
- [16] L.L. Hench, J.K. West, B.F.Z.R. Ochoa, in: *SPIE – the International Society for Optical Engineering*, SPIE, San Diego, California, 1990.
- [17] A. Bouajaj, M. Ferrari, M. Montagna, *J. Sol–Gel Sci. Technol.* 8 (1997) 391.